Genomic analysis reveals a polygenic architecture of antler morphology in wild red deer (Cervus elaphus)

Received: 11 May 2021 | Revised: 26 November 2021 | Accepted: 1 December 2021

DOI: 10.1111/mec.16314

ORIGINAL ARTICLE

MOLECULAR ECOLOGY WILEY

Genomic analysis reveals a polygenic architecture of antler morphology in wild red deer (*Cervus elaphus*)

Lucy Peters[1] | Jisca Huisman[1] | Loeske E. B. Kruuk[1,2] | Josephine M. Pemberton[1] | Susan E. Johnston[1]

[1]Institute of Evolutionary Biology, School of Biological Sciences, University of Edinburgh, Edinburgh, UK

[2]Research School of Biology, The Australian National University, Canberra, ACT, Australia

Correspondence
Lucy Peters and Susan E. Johnston, Institute of Evolutionary Biology, School of Biological Sciences, University of Edinburgh, Edinburgh EH9 3FL, UK.
Emails: lucy.peters@inrae.fr and susan.johnston@ed.ac.uk

Funding information
Natural Environment Research Council; European Research Council; Royal Society University Research Fellowship

Abstract

Sexually selected traits show large variation and rapid evolution across the animal kingdom, yet genetic variation often persists within populations despite apparent directional selection. A key step in solving this long-standing paradox is to determine the genetic architecture of sexually selected traits to understand evolutionary drivers and constraints at the genomic level. Antlers are a form of sexual weaponry in male red deer (*Cervus elaphus*). On the island of Rum, Scotland, males with larger antlers have increased breeding success, yet there has been no evidence of any response to selection at the genetic level. To try and understand the mechanisms underlying this observation, we investigate the genetic architecture of ten antler traits and their principal components using genomic data from >38,000 SNPs. We estimate the heritabilities and genetic correlations of the antler traits using a genomic relatedness approach. We then use genome-wide association and haplotype-based regional heritability to identify regions of the genome underlying antler morphology, and an empirical Bayes approach to estimate the underlying distributions of allele effect sizes. We show that antler morphology is highly repeatable over an individual's lifetime, heritable and has a polygenic architecture and that almost all antler traits are positively genetically correlated with some loci identified as having pleiotropic effects. Our findings suggest that a large mutational target and genetic covariances among antler traits, in part maintained by pleiotropy, are likely to contribute to the maintenance of genetic variation in antler morphology in this population.

KEYWORDS
ecological genetics, genomics/proteomics, mammals, quantitative genetics, sexual selection

1 | INTRODUCTION

Sexually selected traits show great variety and complexity across the animal kingdom, ranging from morphology and behaviours that increase attractiveness to the opposite sex, to traits which increase intersexual competitiveness for access to mates (Andersson, 1994). Such traits are frequently under directional strong selection (Kingsolver et al., 2001), with phenotypic differences between related species suggesting that they can evolve rapidly, with downstream consequences for other phenomena such as adaptation, speciation and extinction probability (Lorch et al., 2003; Martínez-Ruiz & Knell, 2017; Ritchie, 2007; Servedio & Bürger, 2014; Wilkinson et al., 2015). Theory predicts that such strong sexual selection will reduce genetic variation within populations, yet empirical studies

often show that sexually selected traits have substantial underlying genetic variation despite evidence of selection (Kotiaho et al., 2001; Kruuk et al., 2002; Pomiankowski & Moller, 1995; Svensson & Gosden, 2007). This contradiction presents an evolutionary paradox, for which several explanations have been proposed. These include differences in selection between the sexes, developmental stages or environmental conditions (Barson et al., 2015; Bourret et al., 2017), phenotypic plasticity (Charmantier & Gienapp, 2014), condition dependence (Dugand et al., 2019) and trade-offs with survival (Johnston et al., 2013). Some of these observations could be due to genetic correlations between traits under opposing selection pressures and linkage disequilibrium between alleles at causal loci and deleterious alleles (Connallon & Hall, 2018; Lande, 1982; Lande & Arnold, 1983). Quantitative genetic studies have provided some insight into these different explanations, through estimating the relative contributions of genetic (i.e. the heritability, h^2) and environmental effects to phenotypic variance, as well as examining phenotypic and genetic correlations with other traits, including fitness (Emlen, 1994; Griffith et al., 1999; Kruuk et al., 2002; Robinson et al., 2006). However, a key limitation of most studies to date is that the genetic architecture of secondary sexual traits is generally unknown—that is, the underlying loci, their number, distribution and relative effect sizes, and the extent of pleiotropy, epistasis and other interactions (Chenoweth & McGuigan, 2010; Timpson et al., 2018). By identifying the genetic architecture of secondary sexual traits, we can better understand the underlying molecular mechanisms and evolutionary processes that drive their variation (Dobzhansky, 1971; Kuijper et al., 2012; Lewontin, 1974; Wilkinson et al., 2015).

Recent genomic advances in natural populations have led to a number of studies characterizing genetic architectures using genome-wide association studies (GWAS, reviewed in Santure & Garant, 2018). Yet, relatively few studies exist for sexually selected traits, with much of the focus on discrete traits with Mendelian or relatively simple genetic architectures (Barson et al., 2015; Hendrickx et al., 2021; Johnston et al., 2011). In these rare cases, mapping specific genomic variants associated with sexual trait variation can allow investigation of sex, age and environment-specific effects at individual loci. As such, they have revealed compelling cases of heterozygote advantage due to trade-offs between reproductive success and survival (Johnston et al., 2013), or due to differences in optimal trait expression between the sexes (Barson et al., 2015). However, in most cases, secondary sexual traits are likely to have oligogenic or polygenic architectures (i.e. moderate to large numbers of underlying loci), particularly in cases where they are condition dependent (Rowe & Houle, 1996). As the number of loci increases and their relative effect sizes decrease, it becomes more difficult to implicate individual loci in trait variation; for example, in analysis of heights of people of European ancestry, only a fraction of the loci underpinning variation has been identified (Yengo et al., 2018). On the other hand, being able to determine that a trait has a polygenic architecture can still shed light on how sexual traits evolve for the following reasons. First, polygenic traits present a large mutational target, contributing to the maintenance of genetic variance via the introduction of new variants (Rowe & Houle, 1996). Second, allele frequency changes at a great number of loci caused by selection is expected to result in a rapid change in trait mean and thus trait evolution. This evolutionary response to selection is then sustained by the aforementioned large mutational input so that the distribution of genetic effects and thus genetic variance is left unperturbed (Barton et al., 2017; Sella & Barton, 2019). Third, pleiotropy and/or linkage between loci could maintain variation through conflicts between traits sharing a similar or linked polygenic architecture (Morrissey et al., 2012; Ruzicka et al., 2019; Teplitsky et al., 2014). Therefore, studies of sexual traits should aim to identify specific genetic variants with large effects on phenotype and should also aim to determine the distribution of polygenic effect sizes and the degree to which these underlying loci are shared between traits. This will not only shed light on potential evolutionary processes and mechanisms in empirical studies, but will also inform the mechanistic details of theoretical models to allow better assumptions to account for the complexities of natural populations (McNamara & Houston, 2009; Wilkinson et al., 2015).

Antlers are a form of sexual weaponry in deer (Cervidae) that are generally only present in males and are shed and regrown annually (Davis et al., 2011). They are used as weaponry in intermale competition for access to females, with larger antlers often associated with increased reproductive success (Kruuk et al., 2002; Malo et al., 2005). Antler weights and dimensions are often moderately heritable in both wild and captive populations (Lukefahr & Jacobson, 1998; Williams et al., 1994; Wang et al., 1999; Van Den Berg & Garrick, 1997; Kruuk et al., 2002, Kruuk et al., 2014; Jamieson et al., 2020). In male red deer (*Cervus elaphus*) on the island of Rum, Scotland, there is directional selection for increased antler weight and number of antler points (known as "form"). Both traits are substantially heritable ($h^2 = 0.38$ and 0.24, respectively) and positively genetically correlated, but no phenotypic response to selection has been observed over a 30-year study period (Kruuk et al., 2002, 2014). Using annual measures of breeding success, quantitative genetic analysis indicates that the selection gradients on the genetic components were not different from zero (for weight) and negative (for form), while the environmental components of selection were both positive (Kruuk et al., 2002, 2014). This suggests that the apparent phenotypic selection for increased antler weight is mainly driven by environmental associations, with males who had experienced favourable environmental conditions having both larger antlers and individual breeding success. In contrast, antler morphology would be constrained by the zero or negative genetic selection gradients (indicative of antagonistic selection at the genetic level), or genetic associations with one or more unknown traits. These results indicate that genetic constraints may contribute to the maintenance of genetic variance. However, to better understand the mechanisms maintaining genetic variance, a logical next step is to determine the genetic architecture of antler morphology. Further, as antlers present a multidimensional

phenotype, adding more information from different measures may contribute to our understanding of potential evolutionary conflict and constraints within the antler and may allow us to characterize the specific genetic variants underpinning heritable variation (Chenoweth & McGuigan, 2010).

In this study, we used an extensive antler morphology data set with 948–3972 observations in 336–891 unique males and genomic data from 38,000 polymorphic SNPs to estimate the heritability and genetic correlations of ten antler traits using genomic relatedness matrices (VanRaden, 2008). We then use genome-wide association and haplotype-based regional heritability to identify regions of the genome underlying antler morphology (Bush & Moore, 2012; Nagamine et al., 2012), and an empirical Bayes approach to estimate the underlying distributions of allele effect sizes (Stephens, 2016). We show that antler morphology is heritable with a polygenic architecture and that almost all antler traits are positively genetically correlated and that some loci can be identified as having pleiotropic effects. Our findings suggest that genetic variation in antler morphology is maintained via a large mutational target and pleiotropy with traits sharing similar complex polygenic architectures in the red deer population.

2 | METHODS

2.1 | Study system

The red deer study population is situated in the North Block of the Isle of Rum, Scotland (57°02′N, 6°20′W), and has been subject to individual monitoring since 1971 (Clutton-Brock et al., 1982). Deer calves are marked with ear tags shortly after birth to enable recording of detailed life histories of individuals. DNA is routinely extracted from neonatal ear punches, postmortem tissue and/or cast antlers (see Huisman et al., 2016). A pedigree of 4515 individuals is available for the population, constructed using single nucleotide polymorphism (SNP) data in the R package Sequoia (Huisman, 2017). Research was conducted following approval of the University of Edinburgh's Animal Welfare and Ethical Review Body and under appropriate UK Home Office licences.

2.2 | Antler measures

Male red deer cast and regrow their antlers every year from the age of one or two (Kruuk et al., 2002). Ten antler measures are routinely taken from cast antlers and antlers from deceased individuals between 1971 and 2017 (see Figure 1 and Table 1 for full details and sample sizes of each measure). All measures of length were taken following the curve of the antler, and measures of circumference were taken at the narrowest point between antler tines (points). Total antler length was defined as the distance from the coronet (base) to the furthest point of the antler. All length and circumference measures were taken in centimetres. Antler weight was measured as the total dry mass of the antler in grams. Antler form was defined as the number of tines, and as this trait can be determined from observations in the field, it has the greatest sample size (3972 observations from 891 stags). Where measurements from both the left and right antlers were available, the mean was taken. Individual measurements were excluded if the antler part was broken and antler weight was discarded if any part of the antler was broken. Only antlers from stags aged 3 years or older were considered, as cast antlers recovered in the field can be reliably assigned to known individuals by their shape from this age onwards (Kruuk et al., 2002, 2014), as has been confirmed by genetic analysis (Huisman et al., 2016). Previous quantitative genetic analyses (i.e. estimation of trait heritabilities) have been conducted in the same population on antler length, weight, coronet circumference, brow length and form (Kruuk et al., 2002, 2014). The current study adds five additional antler measures, as well as more observations per antler measurement, for example, 1003 observed antler weight observations compared to 706 in Kruuk et al. (2014).

2.3 | Genomic data set

DNA samples from 2870 individuals have been genotyped at 51,248 SNP markers (Huisman et al., 2016) on the Cervine Illumina BeadChip (Brauning et al., 2015) using an Illumina genotyping platform and Illumina GenomeStudio software (Illumina Inc., San Diego, CA, USA). All SNPs on the Cervine Illumina BeadChip are named based on their synteny with the cattle genome BTA vUMD 3.0 (e.g. SNP ID

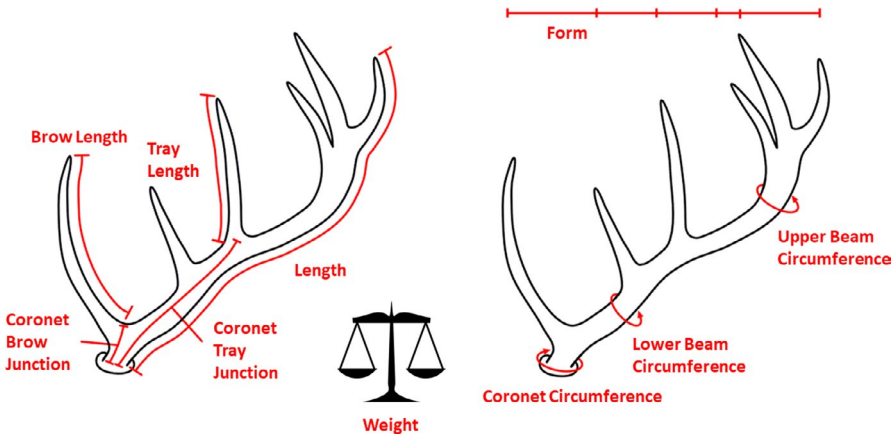

FIGURE 1 A schematic of the antler measures used in this study (measured in *cm*). All traits were measured in *cm*, with the exception of antler weight (measured in *g*) and form, which is the total number of points on an antler. Further details for each measurement are given in the main text and in Table 1

TABLE 1 Summary statistics of all 10 antler measures as shown in Figure 1 in SNP genotyped males

Trait	N Obs	N IDs	Mean	SD	Minimum	Maximum
Antler length	1060	444	65.168	12.029	15.50	93.80
Coronet circumference	1224	471	15.626	2.013	4.60	21.70
Lower beam circumference	1204	460	10.504	1.533	4.30	18.00
Upper beam circumference	1123	436	9.446	1.358	5.85	15.00
Coronet–Brow junction	1162	466	5.720	1.025	3.00	9.80
Coronet–tray junction	1184	455	27.313	5.398	7.30	55.90
Brow length	1139	457	20.568	5.461	1.00	35.20
Tray length	948	388	14.484	4.177	1.00	27.40
Antler weight	1003	336	649.858	243.098	55.00	1505.50
Form (total number of points)	3972	891	4.498	1.072	1.00	8.00

Note: N Obs is the number of observations; *N IDs* is the number of unique individuals for each measure. All lengths and circumferences were measured in *cm*; weight was measured in *g*. *SD* denotes the standard deviation on the raw date (not corrected for age).

cela1_red_15_1479373 is orthologous to position 1479373 on cattle chromosome 15). In addition, a linkage map specific to the Rum population is available, with 38,083 SNPs assigned to linkage groups corresponding to the 33 deer autosomes and X chromosome (Johnston et al., 2017). The SNP positions in both the GWAS and regional heritability analyses were based on the linkage map. Quality control was carried out in PLINK v1.9 (Chang et al., 2015) with the following thresholds: SNP genotyping success >0.99, minor allele frequency >0.01 and individual genotyping success >0.99. Further quality control of mapped SNPs and X-linked markers (i.e. heterozygous state in males) was conducted using the *check.marker* function with default thresholds in the R library GenABEL v1.80 in R v3.4.2 (Aulchenko et al., 2007). The final SNP data set consisted of 2138 individuals and 38,006 markers. Genome-wide linkage disequilibrium (LD) was calculated between all SNPs within 1Mb of each other using Spearman's rank correlation (r^2). Based on a linear regression of r^2 on the log base pair distance between SNPs, LD decayed from ~0.204 at a relatively low rate of 0.031 r^2 per Mb (SE = 5.56×10^{-4}, Figure S1).

2.4 | Principal components of antler measures

A principal component analysis (PCA) was conducted to create a second data set combining information from the different antler measures, while also increasing the differentiation among the different principal components (PCs). As PCA does not allow for missing data, we imputed missing antler measures using the Bayesian *bpca* algorithm in the packages pcaMethods v1.7 in R v3.4.2 (Oba et al., 2003; Stacklies & Redestig, 2018). We used the default settings which assumes a flat prior distribution for imputation, and the most appropriate number of PCs was determined using the *kEstimate* function. To improve imputation accuracy, 'form' was divided into lower and upper values for each antler, to represent the number of tines (branches) on the lower part of the antler ('lower beam' (1–3 tines), 1 and the upper part ('upper beam' (1–5 tines)), respectively, resulting in 11 antler measures. Imputation accuracy was quantified by calculating the error of prediction (*E*) from a complete subset of the data with no missing values and the same subset with randomly missing data at a similar level to the whole data set (~9%). The error of prediction was calculated as follows:

$$E = \sum (V - I)^2 / \sum (V)^2 \quad (1)$$

where *I* refers to the imputed values of the data subset with missing values and *V* to their counterpart in the complete data subset (Stacklies & Redestig, 2018). Our analysis found that the imputation of missing values using a Bayesian PCA approach achieved high accuracy and hence low error ($E = 0.015$). To account for variation among antlers due to age, antler measure values were modelled using a linear model approach (following Pallares et al., 2014). All models had the same structure:

$$y = Age + Age^2 + e \quad (2)$$

where *y* is a vector of the antler measure and *e* is a residual error term. Age effects were fitted as a fixed quadratic term to account for the nonlinear change in antler measures with age (see also Nussey et al., 2009 and Kruuk et al., 2002). All antler measures were modelled using a Gaussian distribution. All models were fitted using the *lm* function in R v3.4.2. The residuals of these models were then used in a standard PCA using the *prcomp* function in R and the scores of the PCs used as trait values in the downstream analysis.

2.5 | Estimating heritability using the animal model

All antler measures and PCs were modelled using a restricted maximum-likelihood (REML) approach within the mixed 'animal model' framework (Henderson, 1975) in asreml-R v4.0 (Butler et al., 2009) in R v3.4.2. The animal model estimates the effect sizes of fixed effects and partitions phenotypic variance (V_p) into several random effects, including the variance attributed to additive genetic effects (V_A). We wished to compare estimates of *VA* using both pedigree and genomic relatedness information based on genome-wide SNP genotype data. Therefore, all models were carried out estimating

VA in one of two ways: (1) using a numerator relationship matrix *A* based on the pedigree, calculated using the ainv function in ASREML-R; and (2) using a genomic relatedness matrix (GRM) (VanRaden, 2008) calculated using autosomal SNPs (N = 37,271) in the --make-grm function in GCTA v1.24.3 (Yang et al., 2011). The GRM was adjusted to assume similar frequency spectra of genotyped and causal loci with the argument --grm-adj 0. It should be noted that a previous quantitative genetic study of antler traits by Kruuk et al. (2014) estimated *VA* using an older pedigree-derived relatedness matrix based on microsatellite and behavioural data. They also modelled heritabilities using a Bayesian mixed model framework in the R package MCMCGLMM (Hadfield, 2009) due to the inclusion of non-Gaussian fitness data in their study. As the current study focusses on largely Gaussian data, we instead employed the REML approach of ASREML-R throughout as it was more efficient and appropriate for our data.

All 10 antler measures and 11 PCs were modelled in univariate animal models with the following structure:

$$y = X\beta + Z_1 a + Z_r u_r + e \quad (3)$$

where y is a vector of the antler measure or PC; X is an incidence matrix relating individual measures to the vector of fixed effects β; Z_1 and Z_r are an incidence matrices relating individual measures to additive genetic and other random effects respectively; a is a vector of relatedness matrix A or GRM; u_r is a vector of additional random effects; and e is a vector of residual effects. Fixed effects included age in years as a both a linear and quadratic term for the antler measures and an intercept only for the PC models (as age structure was accounted for prior to PC estimation). Random effects included the following: the additive genetic effect; permanent environment (i.e. individual identity) to account for pseudoreplication due to repeated measures in the same individual; and birth year and year of antler growth to account for common environmental effects between individuals. The narrow sense heritability (h^2) was calculated as V_A/V_P, where V_P was defined as the sum of the variance attributed to all random effects, including the residual variance Falconer1996IntroductionGenetics. The significance of fixed effects was calculated with a Wald test, while the significance of the random effects was tested using a likelihood ratio test (LRT) between models with and without random effect of interest (i.e. 2 ×the difference between the model log-likelihoods, assuming a chi-square distribution with 1 degree of freedom).

Bivariate models were run to determine genetic correlations between the 10 antler measures, with the following structure:

$$\begin{bmatrix} y_1 \\ y_2 \end{bmatrix} = \begin{bmatrix} X_1 & 0 \\ 0 & X_2 \end{bmatrix} \begin{bmatrix} \beta_1 \\ \beta_2 \end{bmatrix} + \begin{bmatrix} Z_1 & 0 \\ 0 & Z_2 \end{bmatrix} \begin{bmatrix} a_{a_1} \\ a_{a_2} \end{bmatrix} + \begin{bmatrix} Z_{r_1} & 0 \\ 0 & Z_{r_2} \end{bmatrix} \begin{bmatrix} u_{r_1} \\ u_{r_2} \end{bmatrix} + \begin{bmatrix} e_1 \\ e_2 \end{bmatrix} \quad (4)$$

All variables are as defined in equation (3), with subscripts referring to antler traits 1 and 2, respectively. The pedigree-derived relatedness matrix and the GRM gave very similar estimates for the additive genetic variance in the univariate animal models for estimation of trait heritability (see results section). We decided to use the GRM to model the additive genetic covariance to capture any small deviation of genome-sharing from the expected proportions used by the pedigree based matrix. The genetic correlation r^2 was obtained from the genetic covariance, as $r_a = cov_a(1,2)/\sigma_1\sigma_2$, where $cov_a(1,2)$ is the covariance between traits 1 and 2, and σ represents the respective standard deviations for traits 1 and 2. The significance of r_a was determined using an LRT as above, by comparing the model to another where r_a was constrained to either zero or one.

2.6 | Genome-wide association studies

Genome-wide association studies (GWAS) (Bush & Moore, 2012) were conducted in REPEATABEL v1.1 (Rönnegård et al., 2016) implemented in R v3.4.2. First, the *prefitModel* function was used to fit a linear mixed model (without fixed SNP effects), specifying the same fixed and random effect structure as Equation 3. The resulting covariance matrix of the random effects was then input to the *rGLS* function, which fits each SNP genotype as an additive linear covariate. This approach accounts for population structure by fitting the GRM as a random effect and allows for repeated measures per individual. The significance of each SNP was determining using Wald tests, distributed as chi-square with 1 degree of freedom. These statistics were corrected for potential inflation due to population structure not captured by the GRM by dividing them by the genomic inflation factor λ, defined as the observed median χ^2 statistic divided by the null expectation median χ^2 statistic (Devlin & Roeder, 1999). This was done separately for each antler measure. After correction, the genome-wide significance threshold was set to a p-value of 1.42×10^{-6}, equivalent to $\alpha = 0.05$ after correcting for multiple testing and accounting for nonindependence due to LD between SNP markers (see Johnston et al., 2018).

2.7 | Regional heritability analysis

In addition to GWAS, we used a regional heritability approach to identify regions of the genome associated with antler trait variation. This method uses information from multiple loci to determine the proportion of V_P explained by defined genomic regions, and has increased power to detect variants of small effect sizes and low minor allele frequencies (Nagamine et al., 2012; Yang, Manolio, et al., 2011). Regions were defined using a 'sliding window' approach with SNPs of known position on the Rum deer linkage map (Johnston et al., 2017). Each window was 20 SNPs wide and overlapped the preceding window by 10 SNPs. If the last window in the linkage group contained <20 SNPs because the number of SNPs on the chromosome was not divisible by 20, the last 20 SNPs of that linkage group were taken instead. SNPs in linkage group 34, which corresponds to the X chromosome, were excluded from this analysis, as models using X-linked markers did not converge. This resulted in a total of 3608 genomic windows. The contribution of each genomic region to V_A and V_P for each antler measure and PC was modelled as follows:

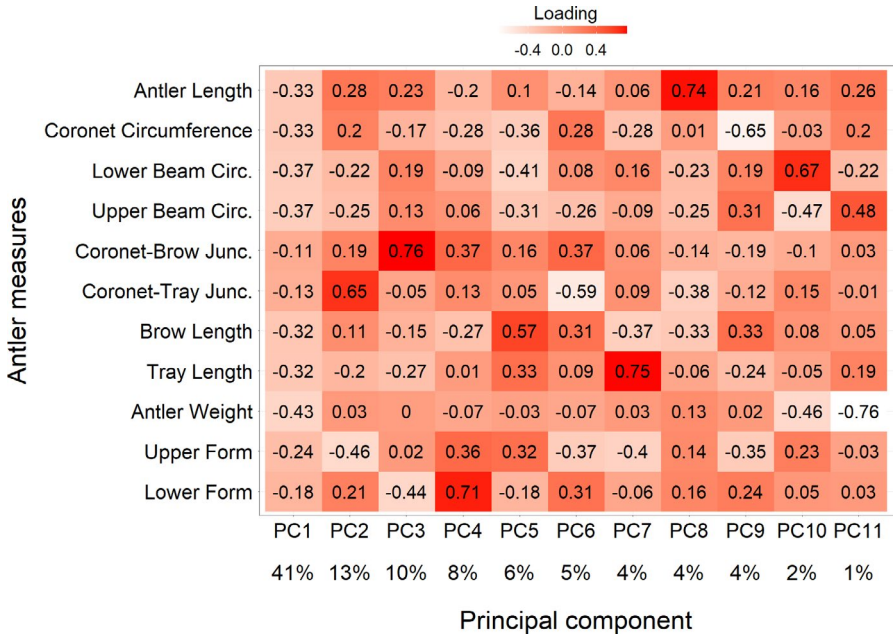

FIGURE 2 Heatmap showing the contribution (as a proportion) of each antler measurement to each of the 11 principal components. The proportion of phenotypic variance explained by each PC is given in percentage along the bottom

$$y = X\beta + Z_1(a - v_i) + Z_2 v_i + Z_r u_r + e \quad (5)$$

with variables defined as in Equation (3), but with the additive genetic components split into two terms: $Z_1(a–v_i)$ and $Z_1 v_i$, where Z_1 is an incidence matrix of the GRM constructed based on all autosomal SNPs excluding those in window i, $(a–v_i)$ is the additive genetic effect excluding the window i; Z_2 is an incidence matrix of the GRM constructed with only the SNPs in window i and v_i is the additive genetic effect of the window i. The significance of an association between a window i and an antler trait was determined using a LRT comparing models containing and omitting the term $Z_2 v_i$. The distribution of χ^2 statistics from the LRTs across all windows was corrected using the genomic control parameter λ, calculated using the same approach as above (Devlin & Roeder, 1999). A genome-wide significance threshold was calculated using a Bonferroni correction, where the α significance level (here 0.05) was divided by the number of effective tests. For this, we divided the number of windows by two to account for the overlap of half the number of total SNPs within each window, resulting in a significance threshold of $p = 2.77 \times 10^{-5}$. As Bonferroni can be a conservative measure, we also used a Benjamini–Hochberg false discovery rate test (Benjamini & Hochberg, 1995) at $\alpha = 0.05$ using the function *p*.adjust in R v3.6.3 for all antler trait and PC analyses *p*-values; this approach gave qualitatively the same results.

2.8 | Estimation of SNP effect size distribution

We investigated the distribution of allele effect sizes and false discovery rates (FDR) for all antler measures and PCs using the *ash* function in the R package ASHR v2.2–32 (Stephens, 2016). This applies "adaptive shrinkage," within an empirical Bayes framework that uses the slopes and standard errors of the additive SNP effects from the GWAS models above to compute a posterior distribution of SNP effect sizes across all loci. This approach estimates the local false discovery rate (*lfdr*), which is the probability that the SNP effect is zero. The significance of a SNP effect was then determined by a local false sign rate (*lfsr*), defined as the probability of making an error when assigning a sign (positive or negative) to an effect, with a cut-off at $\alpha = 0.05$. The prior distribution was specified to be any symmetric unimodal distribution when applying the *lfdr* estimation. The prior distribution was specified to be any symmetric unimodal distribution when applying the lfdr estimation. In order to separate the effects of LD between markers, this analysis was carried out on the full SNP data set and on LD-pruned data sets where the threshold of pairwise r^2 between SNPs was 0.2, 0.5 or 0.8. Pruning was carried out in PLINK v1.9 (Chang et al., 2015) using the --indep-pairwise function, with a window size of 20 SNPs and an overlap of 10 SNPs. This resulted in data sets of 13,459, 30,634 and 35,924 SNPs, respectively.

To better understand and compare the contribution of nonzero effect SNPs on antler phenotypes between the standard animal model and FDR approaches, we re-estimated the effect sizes of the SNP with the highest nonzero effects on each trait within the animal model framework (Equation 3) in ASREML-R v4.0 (Butler et al., 2009). SNP genotype was fit as a three level 325 fixed factor, and significance was tested using a Wald test. Fitting SNP genotype as a factor allowed quantification of the effect size, the dominance deviation and the variance covariance structure of the genotypes, which are needed to estimate the variance attributed to each SNP, calculated as follows (Falconer & Mackay, 1996):

$$V_{SNP} = 2pq(a + d(q - p))^2 \quad (6)$$

where p and q are the allele frequencies of alleles A and B, respectively; a is the additive genetic effect defined as the midpoint between the effect sizes of the genotypes AA and BB; and d is the dominance

deviation defined as the difference between *a* and the effect size of the heterozygote *AB*. The proportion of V_A attributed to a SNP was calculated as the ratio of V_{SNP} to the sum of V_{SNP} and the V_A obtained from an animal model where the SNP effect was omitted. Standard errors of V_{SNP} were estimated using the *deltamethod* function in the R library msm v1.6.7 (Jackson, 2011) in R v3.4.2.

3 | RESULTS

3.1 | Principal component analysis of antler measures

A principal component analysis (PCA) of 11 antler measures resulted in the maximum number of principal components (i.e. 11 PCs). The composition of the PCs showed that PC1, which explained around 41% of the variance, combined approximately equal amounts of information from all 11 measures, while PCs 2 to 11 explained increasingly less variance, mostly representing one or two antler measures (Figure 2). Almost all antler measures were also significantly positively phenotypically correlated (using Pearson's product moment correlation coefficient), except for the correlation of tray length with coronet–tray junction. The phenotypic correlation coefficients ranged from $r = 0.07$ for the correlation of coronet–tray junction with form to $r = 0.85$ for the correlation of lower beam with upper beam circumference (see Table S1).

3.2 | Animal models of antler measures

Antler measures were significantly heritable, with estimates ranging from $h^2 = 0.211$ to 0.436 for the pedigree estimates, and $h^2 = 0.229$ to 0.414 for the genomic estimates (Figure 3; Table 2 and Table S2). Heritability estimates for antler weight, antler length, coronet circumference, brow length and form were generally consistent with previous findings by Kruuk et al. (2014, Figure 3). All antler PCs were also significantly heritable, although estimates decreased substantially for higher order PCs, which explained relatively small proportions of variance in antler morphology (Figure S2, Table S3). For all antler measures and PCs, confidence intervals between pedigree and genomic relatedness estimates were very similar; there was no trend when comparing estimates of h^2 for the same trait, suggesting that both the pedigree and genomic relatedness matrices capture the additive genetic variance to a similar degree in this population. Therefore, all results described from this point onwards are from models fitting a GRM, unless otherwise stated.

The permanent environmental effect (which includes—among others—dominance and epistatic effects) was generally significant for all antler measures, explaining up to 28.0% (upper beam circumference) of the phenotypic variance (Table 2). Year of antler growth explained a significant proportion of phenotypic variance for most antler measures and PCs (Table 2 and Table S3, respectively). Conversely, birth year was not significant for any antler measure or PC; nevertheless, we retained this random effect in all models to account for

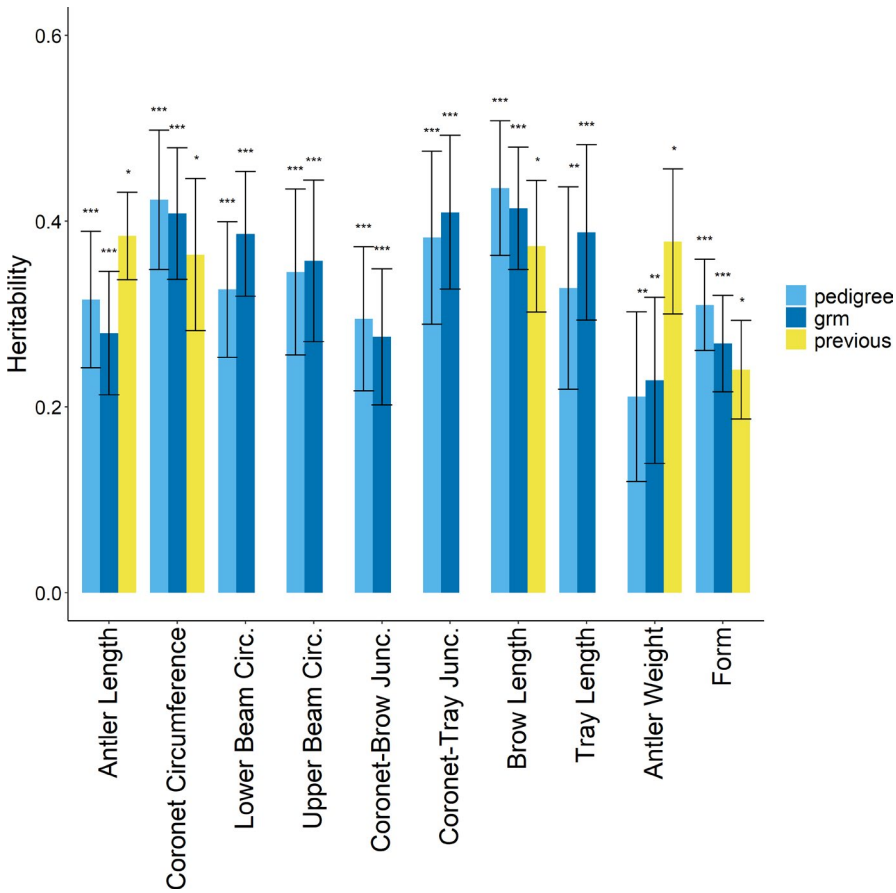

FIGURE 3 Heritability estimates for all 10 antler measures. Both estimates from the pedigree and the GRM models are shown as well as results from a previous study by Kruuk et al. (2014) for antler weight and form. $^*p \le .05$, $^{**}p \le .01$ and $^{***}p \le .001$. Underlying data are provided in Table S2

TABLE 2 Proportions of phenotypic variance (V_P) explained by random effects in animal models of the ten antler measures, from models in which the additive genetic variance was estimated using the GRM. Standard errors are given in brackets. Information on sample sizes and mean measures is provided in Table 1

Trait	V_P	Heritability	Permanent environment	Birth year	Growth year	Residual	Repeatability
Antler Length	61.155	0.279 (0.066)	0.105 (0.058)	1.04E−08 (0.014)	0.222 (0.047)	0.393 (0.035)	0.385
Coronet Circ.	3.047	0.408 (0.071)	0.128 (0.056)	0.018 (0.018)	0.243 (0.047)	0.203 (0.020)	0.554
Lower Beam Circ.	1.323	0.386 (0.067)	0.096 (0.054)	2.22E−07 (1.64E−08)	0.211 (0.042)	0.307 (0.027)	0.483
Upper Beam Circ.	1.084	0.357 (0.087)	0.280 (0.081)	5.16E−08 (0.017)	0.164 (0.035)	0.199 (0.018)	0.637
Coronet–Brow Junc.	0.872	0.275 (0.073)	0.254 (0.068)	0.026 (0.022)	0.152 (0.037)	0.292 (0.025)	0.555
Coronet–tray Junc.	20.930	0.410 (0.083)	0.148 (0.072)	0.001 (0.016)	0.019 (0.009)	0.422 (0.032)	0.559
Brow Length	21.555	0.414 (0.066)	0.068 (0.050)	6.33E−09 (0.013)	0.269 (0.050)	0.250 (0.025)	0.481
Tray Length	13.809	0.388 (0.094)	0.273 (0.088)	7.65E−08 (5.34E−09)	0.028 (0.012)	0.311 (0.028)	0.661
Antler Weight	30727.710	0.229 (0.089)	0.263 (0.086)	0.023 (0.027)	0.252 (0.050)	0.233 (0.025)	0.514
Form	0.907	0.268 (0.052)	0.249 (0.046)	0.024 (0.015)	0.044 (0.011)	0.416 (0.019)	0.541

potential cohort effects (Table 2 and Table S3). Trait repeatabilities, calculated as the sum of contributions from the additive genetic, the permanent environment and birth year components, were high for all antler measures, ranging from 38.5% (antler length) to 66.1% (tray length; Table 2). Age as both linear and quadratic fixed effect terms was significantly associated with all antler measures (Table S4).

3.3 | Genetic correlations between antler measures

Most antler measures were positively genetically correlated, suggesting some degree of shared genetic architecture (Table 3). A high degree of correlation was also reflected in the disproportionate contribution of all antler measures to PC1 (Figure 2). Antler weight was significantly positively genetically correlated with almost all other measures (with the exception of coronet–tray junction), with genetic correlations ranging from $r = 0.40$ for its correlation with coronet–brow junction to $r = 0.94$ for that with upper beam circumference. The only significant negative genetic correlations were observed between coronet–tray junction and tray length, form and lower beam circumference (Table 3). The phenotypic correlation between coronet–tray junction and tray length was nonsignificant and that with form the smallest among all phenotypic correlations; the phenotypic correlation with lower beam circumference however was substantial $r = 0.29$ (see Table S1).

3.4 | Genome-wide and regional heritability studies

No genomic regions were significantly associated with any antler measure or PC using GWAS (Figure 4 and Figure S3, and Tables S5 and S6, respectively). The regional heritability analysis found no regions of the genome significantly associated with any antler measure or PC (Figure 5 and Figure S4, and Tables S7 and S8, respectively), with the exception of PC9, which was significantly associated with three overlapping windows (corresponding to a ~4.4 Mb region) on CEL linkage group 21. The most strongly associated window explained 16.8% (SE = 8.0%) of the phenotypic variance and 66.3% (SE = 22.0%) of the additive genetic variance. However, PC9 accounts for only 4% of overall phenotypic variance among all antler measures (see Figure 2). Homology with the cattle genome (version ARS-UCD1.2) suggested that there are a total of 19 coding regions within the region covered by all three significant windows. Details of SNPs within this region can be found in Table S9 and associated gene ontology (GO) terms can be found in Table S10.

3.5 | Distribution and quantification of SNP effect sizes

A total of 897 unique SNPs had significant nonzero effects across the ten antler measures (Table 4; full results are provided in Table S14). The number of significant nonzero SNPs ranged from 15 SNPs (antler length) to 279 SNPs (lower beam circumference; Table 4), although antler weight and upper beam circumference had no significant nonzero effect SNPs. Several SNPs showed pleiotropic effects; that is, they were associated with more than one measure (Table S14), with the underlying proportion ranging from 6% (coronet–tray junction) to 68% (tray length; Table 4. Lower beam circumference and antler form showed distributions that included more extreme SNPs with large effects on phenotype outside the 5%–95% quantile boundaries, whereas most other measures had more uniformly distributed effect sizes (Table 4). For the 11 antler PCs, only 159 unique SNPs had nonzero effects (Table S13; full results in Table S15). No pleiotropic SNPs were observed, most likely due to the independence of each PC. PC4 and PC9 had no nonzero effect SNP associations. Only about 25% of the 159 SNPs were in common with the 897 SNPs in the antler measure analysis. This was mainly due to the higher order

TABLE 3 Genetic correlations among all 10 antler measurements

	CC	LBC	UBC	CBJ	CTJ	BL	TL	AW	F
AL	0.678 (0.068) ***	0.640 (0.077) ***	0.664 (0.093) ***	0.674 (0.103) ***	0.665 (0.096) ***	0.549 (0.075) ***	0.447 (0.109) ***	0.854 (0.063) ***	0.406 (0.108) ***
CC	–	0.800 (0.054) ***	0.745 (0.084) ***	0.168 (0.109)	0.369 (0.089) ***	0.650 (0.067) ***	0.603 (0.088) ***	0.913 (0.065) ***	0.565 (0.095) ***
LBC	–	–	0.940 (0.024) ***	0.442 (0.102) ***	−0.322 (0.091) ***	0.592 (0.068) ***	0.810 (0.059) ***	0.928 (0.059) ***	0.780 (0.064) ***
UBC	–	–	–	0.266 (0.132)*	−0.179 (0.112)	0.541 (0.073) ***	0.733 (0.069) ***	0.943 (0.059) ***	0.902 (0.041) ***
CBJ	–	–	–	–	0.492 (0.108) ***	−0.079 (0.109)	−0.006 (0.137)	0.396 (0.185)*	−0.163 (0.126)
CTJ	–	–	–	–	–	0.055 (0.065)	−0.713 (0.073) ***	0.188 (0.146)	−0.521 (0.099) ***
BL	–	–	–	–	–	–	0.739 (0.070) ***	0.710 (0.073) ***	0.608 (0.065) ***
TL	–	–	–	–	–	–	–	0.811 (0.082) ***	0.822 (0.064) ***
AW	–	–	–	–	–	–	–	–	0.890 (0.061) ***

Note: Standard errors are given in brackets.

Abbreviations: AL, antler length; AW, antler weight; BL, brow length; CBJ, coronet-beam junction; CC, coronet circumference; CTJ, coronet-tray junction; F, form; LBC, lower beam circumference; TL, tray length; UBC, upper beam circumference.

*$p \leq 0.05$, **$p \leq 0.01$ and ***$p \leq 0.001$.

PCs (PC6 to PC11) sharing no SNP associations with any antler measures, while other PCs had similar or greater numbers of shared and unique SNPs (PC1 and PC2). The LD-pruned data sets yielded lower numbers of nonzero SNPs compared to the full SNP data set, resulting in 299, 806 and 896 unique SNPs across all antler measures at $r^2 = 0.2$, 0.5 and 0.8, respectively. The distribution of nonzero SNPs, SNP effect sizes and the proportions of pleiotropic SNPs for each trait were similar across all data sets, giving qualitatively similar results to the full data set. Full summaries of these results for all antler measures and PCs are provided in Tables S11 and S12.

We examined the contribution of SNPs with the highest nonzero effects in the FDR analysis to the additive genetic and phenotypic variance by fitting the SNP genotypes as a fixed effect within an animal model framework. Some SNPs appear to explain large proportions of overall genetic and phenotypic variance for their respective traits. For example, the SNP cela1_red_8_56767953 explained 29% of the overall additive genetic and 13% of phenotypic variance in coronet circumference (SNP variance = 0.4499, SE = 0.0760), while for PC8 (which is strongly representative of antler length; Figure 2) the marker cela1_red_4_41756873 explained 59% of the additive genetic and 9% of the phenotypic variance (SNP variance = 0.0413, SE = 0.0077). However, we noted that the standard errors of these variance estimates were also large (see Tables S16 and S17 for full results for the antler measures and PCs, respectively). Furthermore, it is likely that effect sizes are overestimated due to the Beavis effect, which describes the inflation of effect sizes of quantitative trait loci, particularly within small sample sizes (Beavis, 1998; Husby et al., 2015; Slate, 2013). Therefore, while we can determine that these SNPs have significantly nonzero effects on phenotype, it remains challenging to determine the precise proportion of the genetic variance they explain.

4 | DISCUSSION

In this study, we have used a genomic approach to determine the genetic architecture of antler morphology in the red deer of Rum. We have shown that antler morphology is heritable and repeatable over an individual's lifetime and that it is likely to be highly polygenic with a moderate degree of shared genetic architecture across different antler traits. Genome-wide association and regional heritability studies failed to identify any genomic regions associated with antler measures and their principal components, with the exception of a single region on linkage group 21 associated with variation in PC9. Most traits were underpinned by SNPs with uniformly small effect sizes, whereas others, such as lower beam and antler form, showed distributions that included some SNPs with larger effects on phenotype. Overall, our findings suggest that antler morphology has a genetic architecture that largely consists many loci of small effect. Here, we discuss how our findings build on previous quantitative genetic studies in the Rum red deer, and how they inform the broader question of the distribution of genetic architectures of sexually selected male weaponry and the consequences for its evolution.

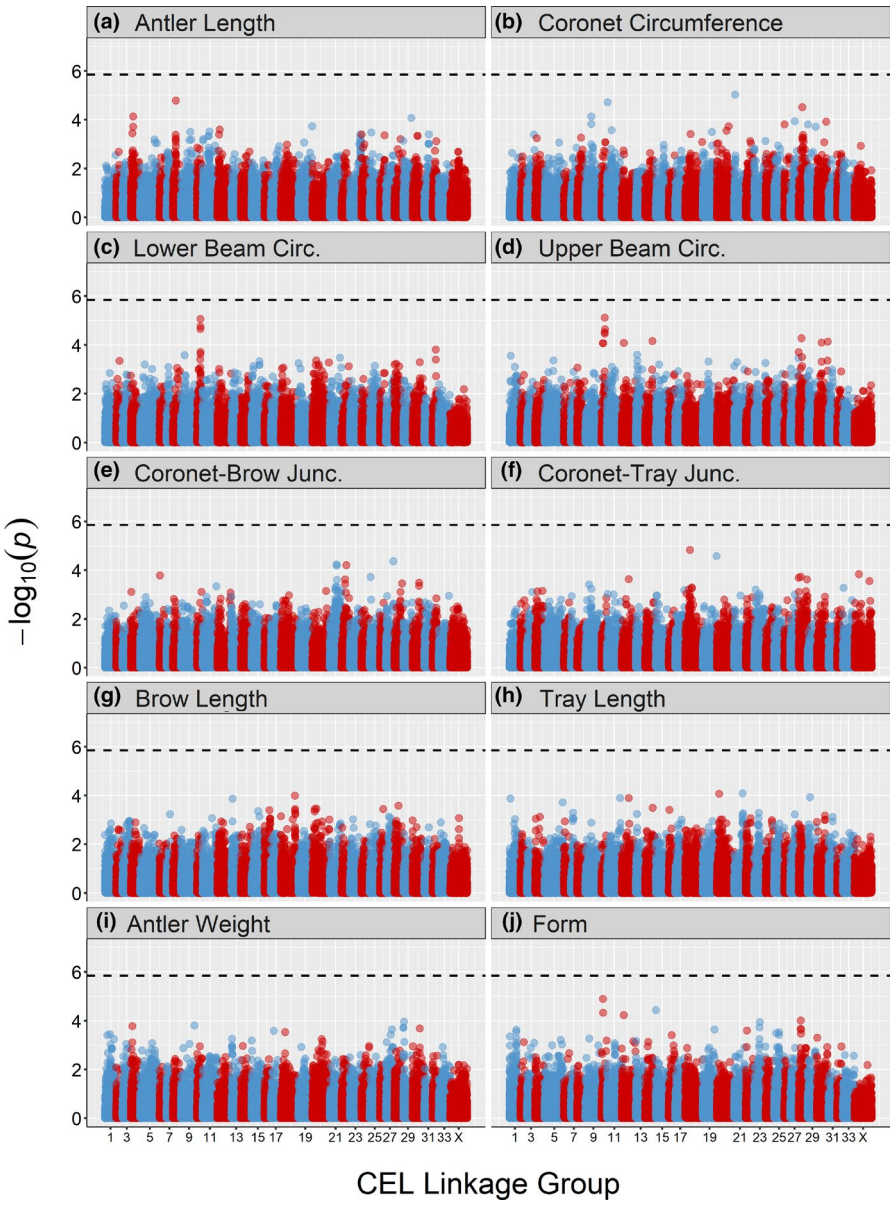

FIGURE 4 Genome-wide association study for antler measures. The dashed line indicates the significance threshold equivalent to $\alpha = 0.05$. Points are colour-coded by chromosome. Underlying data are provided in Table S5

4.1 | Heritability and repeatability of antler morphology

All 10 antler measures were significantly heritable (ranging from 0.229 to 0.414, Table 2) and were similar to previous heritability estimates for antler weight and form in the same population (Kruuk et al., 2014). The strong agreement of estimates from the pedigree and GRM approaches indicates that the SNPs present on the red deer SNP chip are in sufficiently high LD with causative loci to allow accurate estimation of trait heritabilities in this population (Yang et al., 2010; Figure 3). Indeed, LD is maintained at a relatively constant level over a distance of up to 1Mb, after which it starts to slowly decay (Figure S1). All antler traits were also highly repeatable, with between 38.5% and 66.1% of the phenotypic variance explained by additive genetic, permanent environment and birth year effects (after correcting for age). This indicates that antler morphology is temporally stable over an individual's adult life, despite the annual shedding and regrowth of antlers. Similar findings were found for the 11 principal components, with lower order PCs generally exhibiting higher heritabilities and repeatabilities (Table S3); we discuss why we think this is the case in the section on genetic correlations and constraints below. In addition to individual effects, there was significant contribution of the year of growth to phenotypic variance in antler traits, with the exception of the coronet–tray junction, tray length and antler form, explaining 14%–25% of the phenotypic variance (Table 2). These findings support previous work showing that traits under sexual selection can have substantial underlying genetic variation in wild populations (Kruuk et al., 2008; Merila et al., 2001; Pomiankowski & Moller, 1995), of the same magnitude as other morphological traits associated with fitness (Bérénos et al., 2014; Bourret et al., 2017; Johnston et al., 2013; Malenfant et al., 2018).

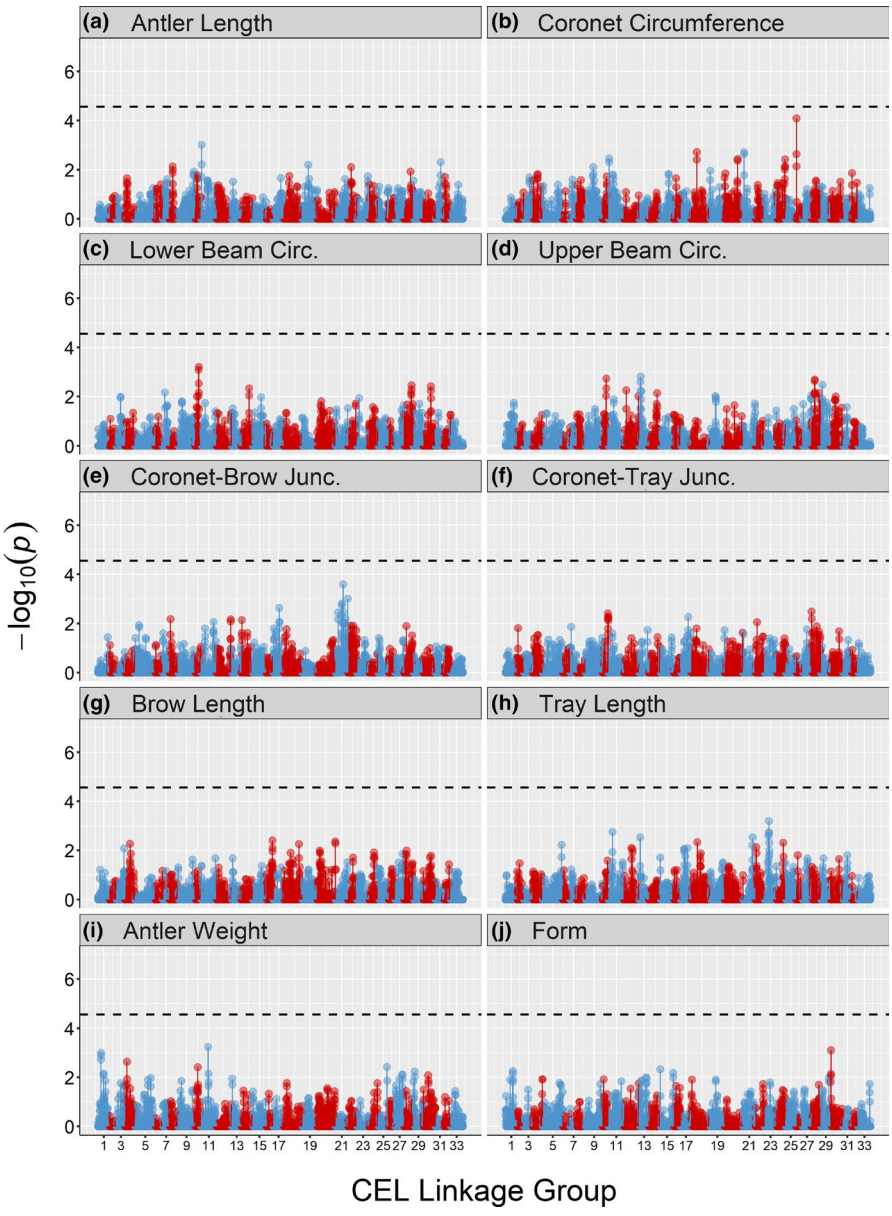

FIGURE 5 Regional heritability analysis for antler measures. The dashed line indicates the significance threshold equivalent to $\alpha = 0.05$. Points are colour-coded by chromosome. Underlying data are provided in Table S7

4.2 | The polygenic architecture of antler morphology

Genome-wide association studies and regional heritability analyses across all antler traits and PCs showed no significant associations, with the exception PC9 (discussed in the next section). Generally, GWAS can only detect loci with moderate to large effects on phenotype and which only partially explain the trait heritabilities, with the remainder termed the "missing heritability" (Golan et al., 2014; Manolio et al., 2009). For example, a meta-analysis of human GWAS found that the heritability attributed to all common SNP variants was significantly higher than that of the SNPs that achieved genome-wide significance (Shi et al., 2016), meaning that large numbers of "nonsignificant" SNPs will contribute to the additive genetic variation. To characterize the genetic architecture beyond GWAS alone, we employed two additional approaches. The first, regional heritability (Nagamine et al., 2012), incorporated the haplotypic diversity within genomic regions. This approach detected a large contribution of defined genomic regions to a single PC, but not to any of the other antler measures or PCs. The second, the empirical Bayes false discovery rate and effect size estimation, incorporated information from the GWAS effect size estimates and their error to show that a substantial number of SNPs had nonzero effects on antler morphology (Stephens, 2016). While this approach provided information whether a SNP had a nonzero effect and the sign of that effect, comparisons with animal models including these SNPs highlight that it remains difficult to determine the precise proportion of the additive genetic variance that these nonzero effects explain. This difficulty may be in part due to the "Beavis effect," where SNP effect sizes are overestimated as a consequence of small sample sizes, which is a common issue in genetic mapping studies of wild populations (Beavis, 1998; Husby et al., 2015; Slate, 2013).

TABLE 4 Summary of SNPs with nonzero effects on antler measures

Antler Measure	N SNPs	Proportion pleiotropic	Maximum effect	Minimum effect	Lower quantile	Upper quantile
Antler Length	15	0.400	0.668	−0.622	−0.619	0.653
Coronet Circ.	56	0.214	0.151	−0.159	−0.152	0.146
Lower Beam Circ.	279	0.136	0.251	−0.151	−0.120	0.144
Upper Beam Circ.	0	-	-	-	-	-
Coronet–Brow Junc.	29	0.138	0.092	−0.084	−0.084	0.091
Coronet–tray Junc.	110	0.055	0.460	−0.490	−0.435	0.441
Brow Length	272	0.081	0.538	−0.532	−0.484	−0.477
Tray Length	6	0.667	0.357	−0.357	−0.355	0.354
Antler Weight	0	-	-	-	-	-
Form	193	0.124	1.018	−0.097	−0.091	0.096

Note: N SNPs is the number of SNPs with nonzero effects. Proportion pleiotropic is the proportion of SNPs with nonzero effects on other antler measures. Maximum and minimum effects are given relative to the data scale (units = cm for lengths, g for weight). Lower and upper quantiles refer to the 5% and 95% boundaries of the effect size distribution, respectively.

The three analyses represent a step-wise process from a traditional approach designed to identify large effect loci (GWAS), a variance-based approach to model haplotypic variation (regional heritability), to an approach designed to model the SNPs as mixture of those with truly zero and truly nonzero effects on phenotype to understand the extent of polygenicity in the data (empirical Bayes false discovery rate). While the results are not mutually exclusive, using these different approaches within the same data set can lend confidence to the nature of the genetic architecture underpinning traits of interest. Taken together, they provide compelling evidence that most aspects of antler morphology have a highly polygenic architecture. This is in line with findings from other studies of wild organisms that have identified polygenic architectures for morphological and life 503 history traits (Berenos et al., 2015; Husby et al., 2015; Pallares et al., 2014; Robinson et al., 2013; Santure et al., 2013). In addition, we modelled antler morphology using both independent measures of antler morphology and a principal component framework to characterize different dimensions of shape variation. An advantage of using both approaches was that it allowed us to identify a greater number of potentially causal loci, which supports the usefulness of this approach when trying to characterize the genetic architecture of a complex morphological trait (such as in Pallares et al., 2014).

4.3 | Genomic regions associated with antler morphology

Three genomic windows within CEL linkage group 21 were associated with PC9 at the genome-wide level (Figure S4). The main contributing antler measure to PC9 was coronet circumference. The region covered by the most highly associated window explained ~66% of the additive genetic variance, representing a large part of the overall heritability estimated using the whole GRM (~19%). The region contains a number of candidate genes among which are gasdermin C (*GSDMC*); MYC proto-oncogene (*MYC*); ArfGAP with SH3 domain, ankyrin repeat and PH domain 1 (*ASAP1*) and cellular communication network factor 4 (*CCN4*). While none of these have previously been implicated in antler morphology, they have associated functions that make them potential candidate genes. Both the enhancer protein *ASAP1* and *CCN4*, which is a type of connective tissue growth factor, are linked to bone ossification and bone cell differentiation in mice (Maeda et al., 2015; Schreiber et al., 2019; The Jackson Laboratory, 2019), processes which are likely to be vital to antler regeneration, rapid growth and the ability of antlers to withstand impact (Goss, 1983). Upregulation of *GSDMC* is implicated in carcinogenesis in mice, as a consequence of an interrupted growth factor signalling pathway (Miguchi et al., 2016) and *MYC* is a potent oncogene that is implicated in many human cancers and promotes rapid tumour cell proliferation (Beroukhim et al., 2010; Lin et al., 2012); recent work suggests that rapid regeneration of bony antlers has evolved by upregulating cell proliferation pathways while suppressing tumorigenesis (Wang et al., 2019).

Despite being linked to compelling candidate gene regions, with our current data it is virtually impossible to determine exactly which genes in this region drive the association with PC9. Furthermore, as PC9 only represents ~4% of the overall phenotypic variance among all antler PCs, we expect effect sizes of causal loci to be very small. Validating the findings for this association would be challenging, as replication of a similar PC in other deer populations would have to consider its main contributing antler measures (e.g. coronet circumference); additionally, the same variants may not be associated with this trait in different populations. A more feasible approach may be to type a higher density of SNP loci to characterize more variation at (or in tight linkage with) potential causal loci in the Rum deer population. While the decay of LD is relatively slow across the genome, the LD between markers within 50kb of one another was ~0.2 (Figure S1), suggesting that there is still additional genetic variation that

remains uncaptured (or "untagged") by the current Cervine SNP chip that may explain more trait variation within this population.

4.4 | Genetic correlations and constraints on antler morphology

Almost all antler traits were positively genetically correlated, with the exception of the coronet–tray junction, which was negatively genetically correlated with tray length, lower beam circumference and antler form. These findings were reflected in the PC analysis, where the PC explaining the most variance in antler morphology (PC1, ~41%) combined equal information from all antler measures, whereas those explaining declining amounts of variation represented one or two antler traits. The empirical Bayes analysis identified varying degrees of marker pleiotropy associated with the antler measures (Table 4) that were consistent with the observed genetic correlations. Nevertheless, there were some exceptions, such as for brow length and antler weight, which both showed strong positive genetic correlations yet had small proportions of shared loci (brow length) or no associated loci at all (antler length). This incongruity may be explained by the large variation in the number of nonzero effect SNPs detected between antler measures, which could be due to differences in the effect size distribution of markers.

The exception to the positive genetic correlations observed above was the case of coronet–tray junction, which was negatively genetically correlated with tray length, lower beam circumference and antler form. A full understanding of this would require further study. One speculative explanation is that there may be a functional constraint: as brow length is phenotypically positively correlated with tray length and coronet–tray junction, the coronet–tray junction may also be larger if both the brow and tray are long to ensure the brow and tray are not crossing. However, if the coronet–tray junction gets too large, it may be harder to interlock antlers with another stag. A more general explanation suggested by Falconer and Mackay (1996) is that negative correlations can arise when traits under opposing directional selection; while some alleles rapidly become fixed, only those with opposing pleiotropic effects will remain for longer at intermediate frequencies, meaning that any remaining genetic covariance after selection will be negative.

The sharing of nonzero SNPs among antler traits suggests that some aspect of genetic correlations between antler traits is due to pleiotropic effects of these shared loci, meaning that they share a functional basis. This is perhaps to be expected, given that these traits are all part of the same structure and tissue type, and pleiotropic mutations are ubiquitous in highly polygenic traits (Lande, 1980). However, as there is extensive LD observed within this population (Figure S1) maintained by significant levels of inbreeding (Coulson et al., 1999; Huisman et al., 2016; Pemberton et al., 1999; Slate et al., 2000), we cannot rule out that SNP sharing and genetic correlations may also be partly explained by signals of linkage disequilibrium between SNPs underpinning different aspects of antler morphology. It is difficult to distinguish between these two mechanisms with certainty without an experimental setting, study replication or extensive simulation, which are beyond the scope of this study. However, our results using LD-pruned data sets suggest that although the absolute number of nonzero SNPs may be overestimated due to LD, the proportion of shared SNPs stayed consistent, supporting the presence of some level of pleiotropy. Furthermore, as we find no marker sharing of nonzero SNPs among PCs, these SNPs conceivably represent a distinct set of genetic loci that affect functionally similar aspects of the antler traits a particular PC represents.

The large heritabilities of individual antler traits suggest there is potential for response to selection, but our results further add to previous findings that constraints at the genetic level may affect how the population may respond to selection (Kruuk et al., 2014). Previous work showed that a large part of genetic variance in antler weight is not available to selection due to the lack of genetic covariance between weight and fitness (Kruuk et al., 2002, 2014). In the current study, antler weight was strongly correlated with most other antler measures at the genetic level, which may likely indicate that large parts of the genetic variance of these antler measures are also unavailable for selection, thus limiting the evolutionary potential of antler morphology despite large heritability estimates. Furthermore, positive genetic correlations can constrain the evolution of traits with large proportions of genetic variances if selection patterns among traits are antagonistic (Teplitsky et al., 2014), and extensive pleiotropy, such as that found in this study, can contribute to maintaining those correlations (Lande, 1980). In the PC analysis, higher order PCs explained much smaller amounts of variation and had very low additive genetic variation. It is possible that these PCs could represent morphologically stable aspects of the antlers, where lower heritabilities could indicate past strong stabilizing selection on the combination of trait aspects represented by that PC. Other studies exploring multivariate sexual selection on a suite of traits found that despite large genetic variance in univariate analyses, there can be very little genetic variance available in the trait composition that is the target of selection (Hunt et al., 2007; Van Homrigh et al., 2007).

4.5 | The maintenance of genetic variation in sexually selected traits

The discovery that the genetic architecture of antler morphology is highly polygenic also suggests that further evolutionary mechanisms may be partially responsible for the maintenance of genetic variation in this trait. As discussed in the introduction, traits with many genes of small effect can present a large mutational target for the introduction of novel genetic variation which can contribute to the genetic variation in a trait (Rowe & Houle, 1996). Consequently, although selection on polygenic traits can lead to rapid changes in trait mean, under the infinitessimal model the distribution of underlying genetic

effects is expected to remain relatively constant, counteracting the loss of genetic variation (Barton et al., 2017; Sella & Barton, 2019). This explanation is plausible in the red deer, as we have shown high polygenicity of antler traits which could provide this mutational target. In addition, we have shown that the genetic architecture of antler traits is likely to possess some level of pleiotropy with each other. This is also expected for traits with polygenic architectures, as many genes affecting a trait will increase their likelihood of being affected by pleiotropy and/or linked selection with loci that are associated with other traits, including those related to fitness (Lande, 1980). This in turn could maintain genetic variation through widespread genomic conflicts and trade-offs (Lande, 1982). Finally, empirical evidence generally supports the idea that sexually selected traits are often condition dependent (Rowe & Houle, 1996). In the case of the deer, we can hypothesize that the combined effects of polygenicity, linkage and pleiotropy may couple antler variation with individual condition, which itself is likely to be driven by the effects of many loci of small effect throughout the genome affecting a wealth of fitness-related traits.

5 | CONCLUSIONS

In this study, we have shown that antler morphology is heritable, has a polygenic genetic architecture and some degree of shared genetic architecture between different antler measures. A single region association is linked to candidate genes that could potentially have an effect on antler morphology, but more work would be required to validate this finding in this and other populations. Future work in this system will integrate knowledge of the genomic architecture of antler morphology with fitness measures to further dissect constraints on trait evolution within this population. Ultimately, our findings corroborate the expectation for a quantitative trait such as multidimensional weaponry traits to conform to a polygenic genetic architecture of many genes with small effects.

ACKNOWLEDGEMENTS

We thank Alison Morris, Sean Morris, Martin Baker, Fiona Guinness, Tim Clutton-Brock and many others for collecting field data and DNA samples over the course of the long-term study. We thank Scottish Natural Heritage for permission to work on the Isle of Rum National Nature Reserve. Andy Arthur kindly provided Figure 1. Philip Ellis prepared samples for DNA extraction and the Wellcome Trust Clinical Research Facility Genetics Core in Edinburgh performed the genotyping. This work made extensive use of the University of Edinburgh Compute and Data Facility (http://www.ecdf.ed.ac.uk/). The long-term project on Rum red deer is funded by the UK Natural Environment Research Council (NERC), and the SNP genotyping was funded by a European Research Council Advanced Grant to J.M.P. L.P is supported by a NERC E3 Doctoral Training Programme PhD Studentship. S.E.J. is supported by a Royal Society University Research Fellowship.

OPEN RESEARCH BADGES

This article has earned an Open Data Badge for making publicly available the digitally-shareable data necessary to reproduce the reported results. The data is available at https://doi.org/10.5061/dryad.612jm643c and all scripts for the analysis are provided at https://github.com/Lucy-Peters/Red_deer_antler_genetic_architecture.

AUTHOR CONTRIBUTIONS

L.P. and S.E.J. designed the study. J.M.P and L.K provided the data. L.P., J.H and S.E.J. analysed the data. L.P. and S.E.J. wrote the first draft of the study and all authors contributed to revisions.

DATA ACCESSIBILITY STATEMENT

All results, information on additional analyses and data underlying the figures in this manuscript are provided as Supplemental Material which is referenced within the text. Table S1 contains the pairwise phenotypic correlations of all antler measures; Table S2 contains the heritability estimates 890 underlying Figure 3 and S2. Table S3 describes the variance components for the PCs as presented for the antler measures in Figure 2. Table S4 contains the estimates of fixed effects from the animal models estimating the heritability of antler measures using the GRM. Tables S5 and S6 contain full detailed results and effect sizes of the genome-wide association studies of the antler measures and PCs, respectively, and Tables S7 and S8 contain the full results of the regional heritability analyses, again of the antler measures and PCs, respectively. Table S9 contains all SNPs within the region covered by the three genomic windows significantly associated with PC9 in the regional heritability analysis, and Table S10 describes a complete list of all genes found in that region homologous to the cattle genome (version ARS-UCD1.2). Tables S11 and S12 contain a summary of effect sizes of SNPs with nonzero effects on antler measures and PCs, respectively, using data sets pruned for LD. Table S13 contains a similar summary of effect sizes of SNPs with nonzero effects on PCs using the full data set. Tables S14 and S15 contain full results and effect sizes for the empirical Bayes FDR correction on GWAS results for all 10 antler measures and PCs, respectively. Tables S16 and S17 contain full detailed results of the mixed animal model estimating effect sizes and variances of the top SNPs after empirical Bayes FDR of the antler measures and PCs, respectively. Figure S1 shows genomic LD decay over a 1 Mb distance. Figure S2 is a plot of heritability estimates for all PCs. Figures S3 and S4 show the results of the genome-wide association studies and regional heritability analyses of the PCs, respectively. Due to their size, Tables S6-S10 and S14-S17 are archived along with data for this study, which includes genomic data after quality control measures, pedigree and linkage map information, and autosomal GRMs, in a Dryad repository (https://doi.org/10.5061/dryad.612jm643c) (Peters et al., 2021). All scripts for the analysis are provided at

https://github.com/Lucy-Peters/Red_deer_antler_genetic_architecture.

ORCID

Lucy Peters https://orcid.org/0000-0002-3640-1493
Jisca Huisman https://orcid.org/0000-0002-9744-7196

REFERENCES

Andersson, M. B. (1994). *Sexual selection*. Princeton University Press.

Aulchenko, Y. S., Ripke, S., Isaacs, A., & Van Duijn, C. M. (2007). GenABEL: An R library for genome wide association analysis. *Bioinformatics*, *23*, 1294–1296. https://doi.org/10.1093/bioinformatics/btm108

Barson, N. J., Aykanat, T., Hindar, K., Baranski, M., Bolstad, G. H., Fiske, P., Jacq, C., Jensen, A. J., Johnston, S. E., Karlsson, S., Kent, M., Moen, T., Niemelä, E., Nome, T., Næsje, T. F., Orell, P., Romakkaniemi, A., Sægrov, H., Urdal, K., … Primmer, C. R. (2015). Sex-dependent dominance at a single locus maintains variation in age at maturity in salmon. *Nature*, *528*, 405–408. https://doi.org/10.1038/nature16062

Barton, N., Etheridge, A., & Véber, A. (2017). The infinitesimal model: Definition, derivation, and implications. *Theoretical Population Biology*, *118*, 50–73. https://doi.org/10.1016/j.tpb.2017.06.001

Beavis, W. D. (1998). QTL analyses: power, precision, and accuracy. In A. H. Paterson (Ed.), *Molecular dissection of complex traits* (pp. 145–162). CRC Press.

Benjamini, Y., & Hochberg, Y. (1995). Controlling the false discovery rate: A practical and powerful approach to multiple testing. *Journal of the Royal Statistical Society: Series B (Methodological)*, *57*, 289–300. https://doi.org/10.1111/j.2517-6161.1995.tb02031.x

Berenos, C., Ellis, P. A., Pilkington, J. G., Lee, S. H., Gratten, J., & Pemberton, J. M. (2015). Heterogeneity of genetic architecture of body size traits in a free-living population. *Molecular Ecology*, *24*, 1810–1830. https://doi.org/10.1111/mec.13146

Bérénos, C., Ellis, P. A., Pilkington, J. G., & Pemberton, J. M. (2014). Estimating quantitative genetic parameters in wild populations: A comparison of pedigree and genomic approaches. *Molecular Ecology*, *23*, 3434–3451. https://doi.org/10.1111/mec.12827

Beroukhim, R., Mermel, C. H., Porter, D., Wei, G., Raychaudhuri, S., Donovan, J., Barretina, J., Boehm, J. S., Dobson, J., Urashima, M., Mc Henry, K. T., Pinchback, R. M., Ligon, A. H., Cho, Y.-J., Haery, L., Greulich, H., Reich, M., Winckler, W., Lawrence, M. S., … Meyerson, M. (2010). The landscape of somatic copy-number alteration across human cancers. *Nature*, *463*, 899–905. https://doi.org/10.1038/nature08822

Bourret, A., Belisle, M., Pelletier, F., & Garant, D. (2017). Evolutionary potential of morphological traits across different life-history stages. *Journal of Evolutionary Biology*, *30*, 616–626. https://doi.org/10.1111/jeb.13031

Brauning, R., Fisher, P. J., & McCulloch, A. F. et al (2015) *Utilization of high throughput genome sequencing technology for large scale single nucleotide polymorphism discovery in red deer and Canadian elk*. bioRxiv.

Bush, W. S., & Moore, J. H. (2012) Chapter 11: Genome-wide association studies. *PLoS Computational Biology*, *8*(12), e1002822.

Butler, D. G., Cullis, B. R., Gilmour, A. R., & Gogel, B. J. (2009) *Mixed models for S language environments: ASReml-R reference manual*.

Chang, C. C., Chow, C. C., Tellier, L. C., Vattikuti, S., Purcell, S. M., & Lee, J. J. (2015). Second-generation PLINK: Rising to the challenge of larger and richer datasets. *GigaScience*, *4*, 7. https://doi.org/10.1186/s13742-015-0047-8

Charmantier, A., & Gienapp, P. (2014). Climate change and timing of avian breeding and migration: Evolutionary versus plastic changes. *Evolutionary Applications*, *7*, 15–28. https://doi.org/10.1111/eva.12126

Chenoweth, S. F., & McGuigan, K. (2010). The genetic basis of sexually selected variation. *Annual Review of Ecology, Evolution, and Systematics*, *41*(41), 81–101. https://doi.org/10.1146/annurev-ecolsys-102209-144657

Clutton-Brock, T., Guiness, F., & Albon, S. (1982). *Red deer. Behaviour and ecology of two sexes*. University of Chicago Press.

Connallon, T., & Hall, M. D. (2018) Genetic constraints on adaptation: A theoretical primer for the genomics era. *Annals of the New York Academy of Sciences*, *1422*(1), 65–87. https://doi.org/10.1111/nyas.13536

Coulson, T., Albon, S., Slate, J., & Pemberton, J. (1999). Microsatellite loci reveal sex-dependent responses to inbreeding and outbreeding in red deer calves. *Evolution*, *53*, 1951. https://doi.org/10.1111/j.1558-5646.1999.tb04575.x

Davis, E. B., Brakora, K. A., & Lee, A. H. (2011) Evolution of ruminant headgear: A review. *Proceedings of the Royal Society B: Biological Sciences*, *278*(1720), 2857–2865. https://doi.org/10.1098/rspb.2011.0938

Devlin, B., & Roeder, K. (1999). Genomic control for association studies. *Biometrics*, *55*, 997–1004. https://doi.org/10.1111/j.0006-341X.1999.00997.x

Dobzhansky, T. (1971). *Genetics of the evolutionary process*, Vol. 139. Columbia University Press.

Dugand, R. J., Tomkins, J. L., & Kennington, W. J. (2019). Molecular evidence supports a genic capture resolution of the lek paradox. *Nature Communications*, *10*, 1–8. https://doi.org/10.1038/s41467-019-09371-y

Emlen, D. J. (1994). Environmental control of horn length dimorphism in the beetle *Onthophagus acuminatus* (Coleoptera: Scarabaeidae). *Proceedings of the Royal Society B-Biological Sciences*, *256*, 131–136.

Falconer, D. S., & Mackay, T. F. C. (1996) *Introduction to quantitative genetics* 4th edn. Longman Harlow.

Golan, D., Lander, E. S., & Rosset, S. (2014). Measuring missing heritability: Inferring the contribution of common variants. *Proceedings of the National Academy of Sciences of the United States of America*, *111*, 5272–5281. https://doi.org/10.1073/pnas.1419064111

Goss, R. J. (1983). *Deer antlers: Regeneration, function and evolution* 1st edn., (pp. 133–171). Academic Press.

Griffith, S. C., Owens, I. P., & Burke, T. (1999). Environmental determination of a sexually selected trait. *Nature*, *400*, 358–360. https://doi.org/10.1038/22536

Hadfield, J. (2009). MCMC methods for multi-response generalized linear mixed models: The MCMCglmm R package. *Journal of Statistical Software*, *33*, 1–22.

Henderson, C. R. (1975). Best linear unbiased estimation and prediction under a selection model. *Biometrics*, *31*, 423–447. https://doi.org/10.2307/2529430

Hendrickx, F., Corte, Z. D., Sonet, G., Belleghem, S. M. V., Köstlbacher, S., & Vangestel, C. (2021). A *Masculinizing supergene underlies an exaggerated male reproductive morph in a spider*, bioRxiv, p. 2021.02.09.430505.

Huisman, J. (2017). Pedigree reconstruction from SNP data: Parentage assignment, sibship clustering and beyond. *Molecular Ecology Resources*, *17*, 1009–1024. https://doi.org/10.1111/1755-0998.12665

Huisman, J., Kruuk, L. E. B., Ellis, P. A., Clutton-Brock, T., & Pemberton, J. M. (2016). Inbreeding depression across the lifespan in a wild mammal population. *Proceedings of the National Academy of Sciences of the United States of America*, *113*, 3585–3590. https://doi.org/10.1073/pnas.1518046113

Hunt, J., Blows, M. W., Zajitschek, F., Jennions, M. D., & Brooks, R. (2007). Reconciling strong stabilizing selection with the maintenance of genetic variation in a natural population of black field crickets (*Teleogryllus commodus*). *Genetics*, *177*, 875–880.

Husby, A., Kawakami, T., Rönnegård, L., Smeds, L., Ellegren, H., & Qvarnström, A. (2015). Genome-wide association mapping in a wild avian population identifies a link between genetic and phenotypic variation in a life-history trait. *Proceedings of the Royal Society B: Biological Sciences*, *282*(1806), 20150156. https://doi.org/10.1098/rspb.2015.0156

Jackson, C. H. (2011). Multi-state models for panel data: The msm package for *R*. *Journal of Statistical Software*, *38*, 1–28.

Jamieson, A., Anderson, S. J., Fuller, J., Côté, S. D., Northrup, J. M., & Shafer, A. B. (2020). Heritability estimates of antler and body traits in white-tailed deer (*Odocoileus virginianus*) from genomic relatedness matrices. *Journal of Heredity*, *111*, 429–435.

Johnston, S. E., Gratten, J., Berenos, C., Pilkington, J. G., Clutton-Brock, T. H., Pemberton, J. M., & Slate, J. (2013). Life history trade-offs at a single locus maintain sexually selected genetic variation. *Nature*, *502*, 93–95. https://doi.org/10.1038/nature12489

Johnston, S. E., Huisman, J., Ellis, P. A., & Pemberton, J. M. (2017). A high-density linkage map reveals sexual dimorphism in recombination landscapes in red deer (*Cervus elaphus*). *G3*, *7*, 2859–2870.

Johnston, S. E., Huisman, J., & Pemberton, J. M. (2018). A genomic region containing REC8 and RNF212B is associated with individual recombination rate variation in a wild population of red deer (*Cervus elaphus*). *G3*, *8*, 2265–2276.

Johnston, S. E., McEWAN, J. C., Pickering, N. K., Kijas, J. W., Beraldi, D., Pilkington, J. G., Pemberton, J. M., & Slate, J. (2011). Genome-wide association mapping identifies the genetic basis of discrete and quantitative variation in sexual weaponry in a wild sheep population. *Molecular Ecology*, *20*, 2555–2566. https://doi.org/10.1111/j.1365-294X.2011.05076.x

Kingsolver, J. G., Hoekstra, H. E., Hoekstra, J. M., Berrigan, D., Vignieri, S. N., Hill, C. E., Hoang, A., Gibert, P., & Beerli, P. (2001). The strength of phenotypic selection in natural populations. *American Naturalist*, *157*, 245–261. https://doi.org/10.1086/319193

Kotiaho, J. S., Simmons, L. W., & Tomkins, J. L. (2001). Towards a resolution of the lek paradox. *Nature*, *410*, 684–686. https://doi.org/10.1038/35070557

Kruuk, L. E. B., Clutton-Brock, T., & Pemberton, J. M. (2014) Case study: quantitative genetics and sexual selection of weaponry in a wild ungulate. In A. Charmantier, D. Garant, & L. E. B. Kruuk (Eds.), *Quantitative genetics in the wild* 1st edn., chap. 10, (pp. 160–176). Oxford University Press.

Kruuk, L. E. B., Slate, J., Pemberton, J. M., Brotherstone, S., & Clutton-Brock, T. H. (2002). Antler size in red deer: Hertability and selection but no evolution. *Evolution*, *56*, 1683–1695.

Kruuk, L. E. B., Slate, J., & Wilson, A. J. (2008). New answers for old questions: The evolutionary quantitative genetics of wild animal populations. *Annual Review of Ecology Evolution and Systematics*, *39*, 525–548. https://doi.org/10.1146/annurev.ecolsys.39.110707.173542

Kuijper, B., Pen, I., & Weissing, F. J. (2012) A guide to sexual selection theory. *Annual Review of Ecology, Evolution, and Systematics*, *43*(1), 287–311. https://doi.org/10.1146/annurev-ecolsys-110411-160245

Lande, R. (1980). The genetic covariance between characters maintained by pleiotropic mutations. *Genetics*, *94*, 203–215. https://doi.org/10.1093/genetics/94.1.203

Lande, R. (1982). A quantitative genetic theory of life history evolution. *Ecology*, *63*, 607–615. https://doi.org/10.2307/1936778

Lande, R., & Arnold, S. J. (1983). The measurement of selection on correlated characters. *Evolution*, *37*, 1210. https://doi.org/10.1111/j.1558-5646.1983.tb00236.x

Lewontin, R. (1974). *The genetic basis of evolutionary change*, Vol. 560. Columbia University Press.

Lin, C. Y., Lovén, J., Rahl, P. B., Paranal, R. M., Burge, C. B., Bradner, J. E., Lee, T. I., & Young, R. A. (2012). Transcriptional amplification in tumor cells with elevated c-Myc. *Cell*, *151*, 56–67. https://doi.org/10.1016/j.cell.2012.08.026

Lorch, P. D., Proulx, S., Rowe, L., & Day, T. (2003). Condition-dependent sexual selection can accelerate adaptation. *Evolutionary Ecology Research*, *5*, 867–881.

Lukefahr, S. D., & Jacobson, H. A. (1998). Variance component analysis and heritability of antler traits in white-tailed deer. *The Journal of Wildlife Management*, *62*, 262. https://doi.org/10.2307/3802287

Maeda, A., Ono, M., Holmbeck, K., Li, L. I., Kilts, T. M., Kram, V., Noonan, M. L., Yoshioka, Y., McNerny, E. M. B., Tantillo, M. A., Kohn, D. H., Lyons, K. M., Robey, P. G., & Young, M. F. (2015). WNT1-induced secreted protein-1 (WISP1), a novel regulator of bone turnover and Wnt signaling. *Journal of Biological Chemistry*, *290*, 14004–14018. https://doi.org/10.1074/jbc.M114.628818

Malenfant, R. M., Davis, C. S., Richardson, E. S., Lunn, N. J., & Coltman, D. W. (2018). Heritability of body size in the polar bears of Western Hudson Bay. *Molecular Ecology Resources*, *18*, 854–866. https://doi.org/10.1111/1755-0998.12889

Malo, A. F., Roldan, E. R., Garde, J., Soler, A. J., & Gomendio, M. (2005). Antlers honestly advertise sperm production and quality. *Proceedings of the Royal Society B: Biological Sciences*, *272*, 149–157. https://doi.org/10.1098/rspb.2004.2933

Manolio, T. A., Collins, F. S., Cox, N. J., Goldstein, D. B., Hindorff, L. A., Hunter, D. J., McCarthy, M. I., Ramos, E. M., Cardon, L. R., Chakravarti, A., Cho, J. H., Guttmacher, A. E., Kong, A., Kruglyak, L., Mardis, E., Rotimi, C. N., Slatkin, M., Valle, D., Whittemore, A. S., … Visscher, P. M. (2009). Finding the missing heritability of complex diseases. *Nature*, *461*, 747–753. https://doi.org/10.1038/nature08494

Martínez-Ruiz, C., & Knell, R. J. (2017). Sexual selection can both increase and decrease extinction probability: Reconciling demographic and evolutionary factors. *Journal of Animal Ecology*, *86*, 117–127. https://doi.org/10.1111/1365-2656.12601

McNamara, J. M., & Houston, A. I. (2009) Integrating function and mechanism. *Trends in Ecology & Evolution*, *24*(12), 670–675. https://doi.org/10.1016/j.tree.2009.05.011

Merila, J., Sheldon, B. C., Kruuk, L. E. B., Merilä, J., Sheldon, B. C., & Kruuk, L. E. B. (2001). Explaining stasis: Microevolutionary studies in natural populations. *Genetica*, *112*, 199–222.

Miguchi, M., Hinoi, T., Shimomura, M. et al (2016). Gasdermin C is upregulated by inactivation of transforming growth factor β receptor type II in the presence of mutated Apc, promoting colorectal cancer proliferation. *PLoS One*, *11*(11), e0166422.

Morrissey, M. B., Walling, C. A., Wilson, A. J., Pemberton, J. M., Clutton-Brock, T. H., & Kruuk, L. E. B. (2012). Genetic analysis of life-history constraint and evolution in a wild ungulate population. *American Naturalist*, *179*, E97–E114. https://doi.org/10.1086/664686

Nagamine, Y., Pong-Wong, R., Navarro, P., Vitart, V., Hayward, C., Rudan, I., Campbell, H., Wilson, J., Wild, S., Hicks, A. A., Pramstaller, P. P., Hastie, N., Wright, A. F., & Haley, C. S. (2012). Localising loci underlying complex trait variation using regional genomic relationship mapping. *PLoS One*, *7*(10), e46501. https://doi.org/10.1371/journal.pone.0046501

Nussey, D. H., Kruuk, L. E., Morris, A., Clements, M. N., Pemberton, J. M., & Clutton-Brock, T. H. (2009). Inter and intrasexual variation in aging patterns across reproductive traits in a wild red deer population. *American Naturalist*, *174*, 342–357. https://doi.org/10.1086/603615

Oba, S., Sato, M., Takemasa, I., Monden, M., Matsubara, K., & Ishii, S. (2003). A Bayesian missing value estimation method for gene expression profile data. *Bioinformatics*, *19*, 2088–2096. https://doi.org/10.1093/bioinformatics/btg287

Pallares, L. F., Harr, B., Turner, L. M., & Tautz, D. (2014). Use of a natural hybrid zone for genomewide association mapping of craniofacial traits in the house mouse. *Molecular Ecology*, *23*, 5756–5770. https://doi.org/10.1111/mec.12968

Pemberton, J. M., Coltman, D. W., Coulson, T. N., & Slate, J. (1999). Using microsatellites to measure the fitness consequences of inbreeding and outbreeding. In D. B. Goldstein, & C. Schlötterer (Eds.), *Microsatellites: Evolution and applications* (pp. 151–164). Oxford University Press.

Peters, L., Huisman, J., Kruuk, L. E., Pemberton, J. M., & Johnston, S. E. (2021). *Genomic analysis reveals a polygenic architecture of antler morphology in wild red deer (Cervus elaphus)*. Dryad [dataset]. https://doi.org/10.5061/dryad.612jm643c

Pomiankowski, A., & Moller, A. P. (1995). A resolution of the lek paradox. *Proceedings of the Royal Society B-Biological Sciences*, *260*, 21–29.

Ritchie, M. G. (2007). Sexual selection and speciation. *Annual Review of Ecology, Evolution, and Systematics*, *38*, 79–102. https://doi.org/10.1146/annurev.ecolsys.38.091206.095733

Robinson, M. R., Pilkington, J. G., Clutton-Brock, T. H., Pemberton, J. M., & Kruuk, L. E. (2006). Live fast, die young: Trade-offs between fitness components and sexually antagonistic selection on weaponry in soay sheep. *Evolution*, *60*, 2168–2181. https://doi.org/10.1111/j.0014-3820.2006.tb01854.x

Robinson, M. R., Santure, A. W., DeCauwer, I., Sheldon, B. C., & Slate, J. (2013). Partitioning of genetic variation across the genome using multimarker methods in a wild bird population. *Molecular Ecology*, *22*, 3963–3980. https://doi.org/10.1111/mec.12375

Rönnegård, L., McFarlane, S. E., Husby, A., Kawakami, T., Ellegren, H., & Qvarnstrom, A. (2016). Increasing the power of genome wide association studies in natural populations using repeated measures - evaluation and implementation. *Methods in Ecology and Evolution*, *7*, 792–799. https://doi.org/10.1111/2041-210X.12535

Rowe, L., & Houle, D. (1996). The lek paradox and the capture of genetic variance by condition dependent traits. *Proceedings of the Royal Society B-Biological Sciences*, *263*, 1415–1421. https://doi.org/10.1098/rspb.1996.0207

Ruzicka, F., Hill, M. S., Pennell, T. M., Flis, I., Ingleby, F. C., Mott, R., Fowler, K., Morrow, E. H., & Reuter, M. (2019). Genome-wide sexually antagonistic variants reveal long-standing constraints on sexual dimorphism in fruit flies. *PLOS Biology*, *17*, e3000244. https://doi.org/10.1371/journal.pbio.3000244

Santure, A. W., De Cauwer, I., Robinson, M. R., Poissant, J., Sheldon, B. C., & Slate, J. (2013). Genomic dissection of variation in clutch size and egg mass in a wild great tit (*Parus major*) population. *Molecular Ecology*, *22*, 3949–3962.

Santure, A. W., & Garant, D. (2018). Wild GWAS-association mapping in natural populations. *Molecular Ecology Resources*, *18*, 729–738. https://doi.org/10.1111/1755-0998.12901

Schreiber, C., Saraswati, S., Harkins, S., Gruber, A., Cremers, N., Thiele, W., Rothley, M., Plaumann, D., Korn, C., Armant, O., Augustin, H. G., & Sleeman, J. P. (2019). Loss of ASAP1 in mice impairs adipogenic and osteogenic differentiation of mesenchymal progenitor cells through dysregulation of FAK/Src and AKT signaling. *PLoS Genetics*, *15*(6), e1008216. https://doi.org/10.1371/journal.pgen.1008216

Sella, G., & Barton, N. H. (2019). Thinking about the evolution of complex traits in the era of genome-wide association studies. *Annual Review of Genomics and Human Genetics*, *20*, 461–493. https://doi.org/10.1146/annurev-genom-083115-022316

Servedio, M. R., & Bürger, R. (2014). The counterintuitive role of sexual selection in species maintenance and speciation. *Proceedings of the National Academy of Sciences of the United States of America*, *111*, 8113–8118. https://doi.org/10.1073/pnas.1316484111

Shi, H., Kichaev, G., & Pasaniuc, B. (2016). Contrasting the genetic architecture of 30 complex traits from summary association data. *The American Journal of Human Genetics*, *99*, 139–153. https://doi.org/10.1016/j.ajhg.2016.05.013

Slate, J. (2013). From beavis to beak color: A simulation study to examine how much QTL mapping can reveal about the genetic architecture of quantitative traits. *Evolution*, *67*, 1251–1262. https://doi.org/10.1111/evo.12060

Slate, J., Kruuk, L. E., Marshall, T. C., Pemberton, J. M., & Clutton-Brock, T. H. (2000). Inbreeding depression influences lifetime breeding success in a wild population of red deer (*Cervus elaphus*). *Proceedings of the Royal Society B: Biological Sciences*, *267*, 1657–1662.

Stacklies, W., & Redestig, H. (2018). *Imputing missing values using the pcaMethods package*.

Stephens, M. (2016). False discovery rates: A new deal. *Biostatistics*, *18*, kxw041. https://doi.org/10.1093/biostatistics/kxw041

Svensson, E. I., & Gosden, T. P. (2007). Contemporary evolution of secondary sexual traits in the wild. *Functional Ecology*, *21*, 422–433. https://doi.org/10.1111/j.1365-2435.2007.01265.x

Teplitsky, C., Tarka, M., Møller, A. P., Nakagawa, S., Balbontín, J., Burke, T. A., Doutrelant, C., Gregoire, A., Hansson, B., Hasselquist, D., Gustafsson, L., de Lope, F., Marzal, A., Mills, J. A., Wheelwright, N. T., Yarrall, J. W., & Charmantier, A. (2014). Assessing multivariate constraints to evolution across ten long-term avian studies. *PLoS One*, *9*(3), e90444. https://doi.org/10.1371/journal.pone.0090444

The Jackson Laboratory (2019). *Mouse Genome Database (MGD) at the Mouse Genome Informatics website*.

Timpson, N. J., Greenwood, C. M., Soranzo, N., Lawson, D. J., & Richards, J. B. (2018). Genetic architecture: The shape of the genetic contribution to human traits and disease. *Nature Reviews Genetics*, *19*(2), 110–124. https://doi.org/10.1038/nrg.2017.101

Van Den Berg, G. H., & Garrick, D. J. (1997). Inheritance of adult velvet antler weights and live weights in farmed red deer. *Livestock Production Science*, *49*, 287–295. https://doi.org/10.1016/S0301-6226(97)00044-4

Van Homrigh, A., Higgie, M., McGuigan, K., & Blows, M. W. (2007). The depletion of genetic variance by sexual selection. *Current Biology*, *17*, 528–532. https://doi.org/10.1016/j.cub.2007.01.055

VanRaden, P. (2008). Efficient methods to compute genomic predictions. *Journal of Dairy Science*, *91*, 4414–4423. https://doi.org/10.3168/jds.2007-0980

Wang, Y. U., Zhang, C., Wang, N., Li, Z., Heller, R., Liu, R., Zhao, Y., Han, J., Pan, X., Zheng, Z., Dai, X., Chen, C., Dou, M., Peng, S., Chen, X., Liu, J., Li, M., Wang, K., Liu, C., … Qiu, Q. (2019). Genetic basis of ruminant headgear and rapid antler regeneration. *Science*, *364*, eaav6335. https://doi.org/10.1126/science.aav6335

Wang, Z., Yang, R. C., Goonewardene, L. A., & Huedepoh, C. (1999). Genetic analysis of velvet antler yield in farmed elk (*Cervus elaphus*). *Canadian Journal of Animal Science*, *79*, 569–571.

Wilkinson, G. S., Breden, F., Mank, J. E., Ritchie, M. G., Higginson, A. D., Radwan, J., Jaquiery, J., Salzburger, W., Arriero, E., Barribeau, S. M., Phillips, P. C., Renn, S. C. P., & Rowe, L. (2015). The locus of sexual selection: Moving sexual selection studies into the post-genomics era. *Journal of Evolutionary Biology*, *28*(4), 739–755. https://doi.org/10.1111/jeb.12621

Williams, J. D., Krueger, W. F., & Harmel, D. H. (1994). Heritabilities for antler characteristics and body weight in yearling white-tailed deer. *Heredity*, *73*, 78–83. https://doi.org/10.1038/hdy.1994.101

Yang, J., Benyamin, B., McEvoy, B. P., Gordon, S., Henders, A. K., Nyholt, D. R., Madden, P. A., Heath, A. C., Martin, N. G., Montgomery, G. W., Goddard, M. E., & Visscher, P. M. (2010). Common SNPs explain a large proportion of the heritability for human height. *Nature Genetics*, *42*, 565–569. https://doi.org/10.1038/ng.608

Yang, J., Lee, H., Goddard, M. E., & Visscher, P. M. (2011). GCTA: A tool for genome-wide complex trait analysis. *The American Journal of Human Genetics*, *88*, 76–82. https://doi.org/10.1016/j.ajhg.2010.11.011

Yang, J., Manolio, T. A., Pasquale, L. R., Boerwinkle, E., Caporaso, N., Cunningham, J. M., de Andrade, M., Feenstra, B., Feingold, E., Hayes, M. G., Hill, W. G., Landi, M. T., Alonso, A., Lettre, G., Lin, P., Ling, H., Lowe, W., Mathias, R. A., Melbye, M., … Visscher, P. M. (2011). Genome partitioning of genetic variation for complex traits using common SNPs. *Nature Genetics*, *43*, 519–U44. https://doi.org/10.1038/ng.823

Yengo, L., Sidorenko, J., Kemper, K. E., Zheng, Z., Wood, A. R., Weedon, M. N., Frayling, T. M., Hirschhorn, J., Yang, J., & Visscher, P. M. (2018). Meta-analysis of genome-wide association studies for height and body mass index in ~700 000 individuals of European ancestry. *Human Molecular Genetics*, *27*, 3641–3649. https://doi.org/10.1093/hmg/ddy271

SUPPORTING INFORMATION

Additional supporting information may be found in the online version of the article at the publisher's website.

How to cite this article: Peters, L., Huisman, J., Kruuk, L. E. B., Pemberton, J. M., & Johnston, S. E. (2021). Genomic analysis reveals a polygenic architecture of antler morphology in wild red deer (*Cervus elaphus*). *Molecular Ecology*, 00, 1–18. https://doi.org/10.1111/mec.16314